Flexural strength of ice from the Rideau Canal: a laboratory investigation

Barrette, Paul; Brassard, Chris

For the publisher's version, please access the DOI link below./ Pour consulter la version de l'éditeur, utilisez le lien DOI ci-dessous.

https://doi.org/10.4224/17506219

CHC CANADIAN HYDRAULICS CENTRE
CENTRE D'HYDRAULIQUE CANADIEN

FLEXURAL STRENGTH OF ICE FROM THE RIDEAU CANAL: A LABORATORY INVESTIGATION

Paul Barrette and Chris Brassard

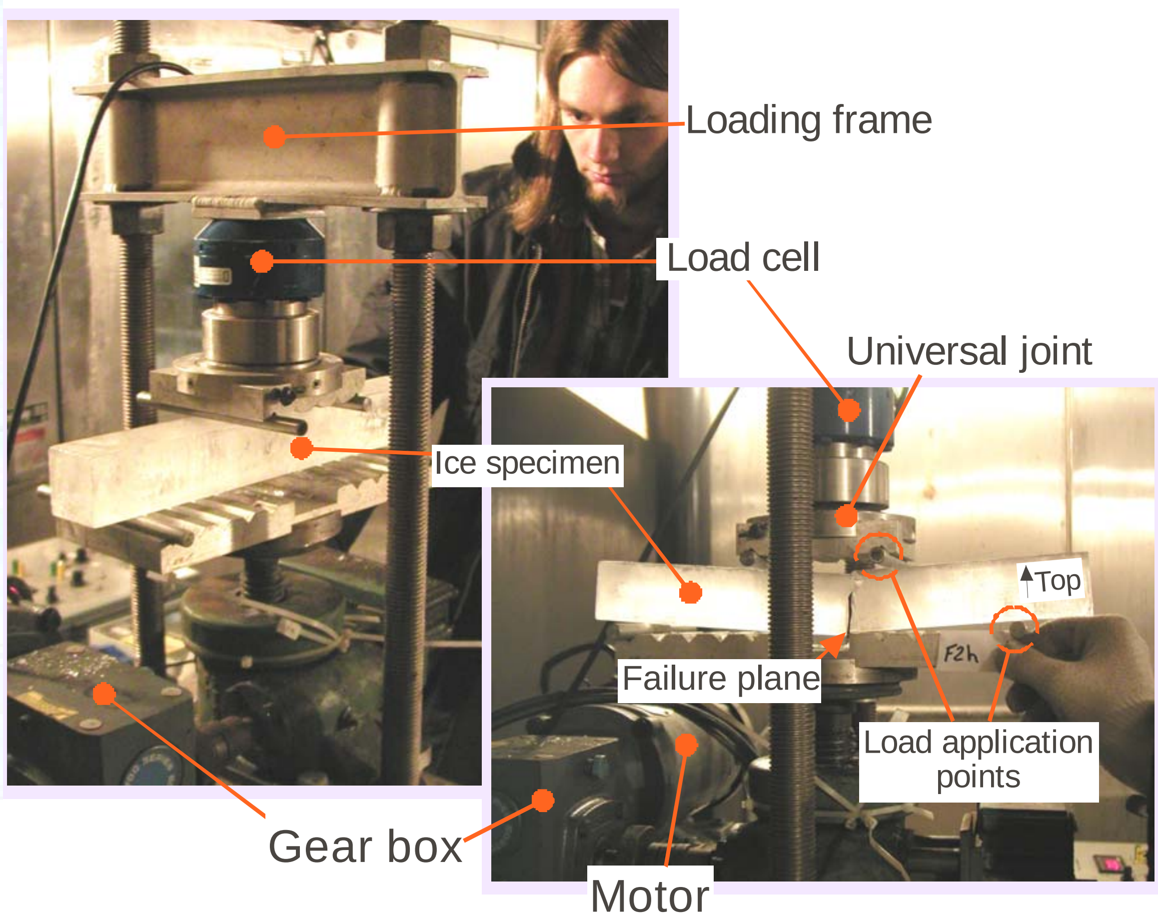

TECHNICAL REPORT
CHC-TR-068

SEPTEMBER 2009

National Research Council Canada
Conseil national de recherches Canada

Ottawa, Canada K1A 0R6
Fax: (613) 952-7679 Internet: http://www.chc.nrc.ca

ABSTRACT

This report contains the results of an experimental study that was conducted in CHC-NRC's cold room facility in July 2009. Its main purpose was to compare the flexural strength of white ice and clear ice that was collected from the Rideau Canal in the winter of 2009, both inside and outside the skateway. A total of 56 successful four-point beam tests were done as part of this test program – 31 on white ice and 25 on clear ice – at three different temperatures: -9.5^{o}C, -5.0^{o}C and -0.5^{o}C. White ice was weaker than clear ice by 36%, 21% and 51% at these test temperatures, respectively. The ice inside the skateway was weaker than that outside of it by 27%, 23% and 37% at these temperatures, respectively. The standard deviations suggest considerable variability in material response.

RÉSUMÉ

Ce rapport présente les résultats d'une étude expérimentale effectuée en chambre froide dans le laboratoire du CHC-CNRC en juillet 2009. Il s'agit d'une étude comparative entre la résistance en flexion de la glace blanche (avec présence d'air) et celle de la glace transparente (sans air). Ces deux types de glace ont été extraits du canal Rideau durant l'hiver 2009, et provenaient de l'intérieur et de l'extérieur de la zone utilisée pour le patinage. Un total de cinquante-six poutres ont été soumises à des essais de flexion 'quatre-points' – 31 sur la glace blanche et 25 sur la glace transparente, et ce, à trois températures différentes : -9.5^{o}C, -5.0^{o}C et -0.5^{o}C. On remarque, à chacune de ces températures, une diminution de 36%, 21% et 51% dans la résistance de la glace blanche par rapport à la glace transparente, ainsi qu'une diminution de 27%, 23% et 37% de la résistance à l'intérieur de la zone de patinage par rapport à l'extérieur. Les écarts types indiquent une dispersion non-négligeable dans le comportement mécanique du matériau.

TABLE OF CONTENTS

FLEXURAL STRENGTH OF ICE FROM THE RIDEAU CANAL: A LABORATORY INVESTIGATION

1 INTRODUCTION

The Rideau Canal in Ottawa is used every winter as a skating rink. In order to ensure the ice cover is safe, it has to be properly managed and maintained. CHC-NRC was contracted out by *BMT Fleet Technology Ltd.* to conduct a laboratory investigation on the flexural strength of that ice and provide additional information on bearing capacity issues. More specifically, the purpose of these investigations was to measure and compare the strength of white ice and clear ice at different temperatures, but otherwise under identical conditions. This was done by resorting to what is known as 'four-point' bending tests. In this report, information on ice harvesting is first presented, followed by the laboratory procedures and the test results.

2 ICE HARVESTING

The ice investigated in this test program was extracted from the Rideau Canal on February 27 2009. Four blocks were cut out from the ice cover that day, all of which had a clear and a white zone (Figure 1). The blocks were labelled E, F, G and H ('A' to 'D' are labels given to blocks from a different location but which were not used in this study). The harvesting site was located at 45^o24.188N and 75^o40.810W (close to the '3.4 km' marker on the skateway). Block E and G were taken from inside the skating zone, at 59 m from the canal's east margin. The thickness was 0.99 m – the upper 27% of it consisted of white ice. Blocks F and H were from outside the skating zone, at 29 m from that same margin. The thickness was 0.71 m – the upper 28% of it consisted of white ice. The water temperature and salinity, obtained from a nearby drill hole, were 0.01^oC and 2.01 parts per thousand, respectively. Air temperature at that time was $+7^o$C, with overcast and rain.

The ice was stored away until testing (for about five months) in a cold room on the CHC premises on Montreal Road in Ottawa, at temperatures ranging from -10^oC to -20^oC.

3 ICE TESTING

3.1 Principles

Mechanical testing of ice (and other crystalline materials) can be done following various modes, notably in compression, in tension, in torsion and in flexure. The flexural mode is the one this study is interested in, since it reflects more closely the load regime that an ice cover undergoes in a bearing capacity situation.

There are two main methods used to test for flexure: cantilever beam and supported beams (Figure 2). Cantilever beam tests better simulate the real events, because these tests can be done in situ (on the ice sheet itself) and at a larger scale. The drawback with this method is that stress concentrations occur at the base of the beam near the failure plane (Frederking and Svec, 1985; Svec *et al.*, 1985). As a result, these tests tend to underestimate flexural strength (Timco and O'Brien, 1994, Fig. 3). As an alternative, beam tests can be done by applying the load either through three points or four points (along the beam's longitudinal cross-section – Figure 2, right). In the first case, failure *must* occur directly below the beam (as shown in the sketch), otherwise the conventional formulation used to derive flexural strength will not be valid. Since ice is a rather heterogeneous material (air voids, microcracks, etc.), it will have a propensity to break at different points. For that reason, a 4-pt configuration is the preferred option, since the load distribution with this configuration is uniform across the entire zone between the two upper load application points. Failure may then occur anywhere within that zone.

The formulation used to determine flexural strength of an ice beam under a four-point loading configuration is

$$\sigma_f = \frac{3FD}{WT^2} \qquad \textit{Eq. 1}$$

where σ_f is the flexural strength, F is the force applied to the upper loading points, D is the separation between the upper loading point and the lower support point, W is the beam width and T is the beam thickness (Figure 3). Note that Eq. 1 is derived from basic concepts in conventional mechanics, which assume that the material is rigorously uniform. This is generally not the case with ice, as mentioned above, but these concepts are still used in ice engineering. They normally lead to a fairly wide data scatter, which is why it is wise to repeat the same test a number of times.

The strain rate can be determined from

$$\frac{d\varepsilon}{dt} = \frac{TR}{\left(LD - \frac{4}{3}D^2\right)} \qquad \textit{Eq. 2}$$

where $d\varepsilon/dt$ is the strain rate, R is the loading rate (the speed at which the indentor moves toward the specimen) and L is the distance between the two lower supports.

3.2 Beam preparation

With an electric chainsaw, each of the four large blocks harvested from the field was cut into smaller, more manageable pieces. These pieces were then labelled with a number (*e.g.* E1, E2, etc.). Some were made from white ice, others from clear ice. A band saw was used to further trim these pieces into the final beam dimensions, which were 50 mm x 50 mm in cross-section and 400 mm in length. Variations in these values were within about 2 mm for the cross-section dimensions, and within 10-20 mm for the length. Several beams could be extracted from each piece, and these were labelled with a letter (*e.g.* E1a, E1b, …). The top of the ice sheet was monitored throughout this process, and was indicated onto each beam. (There was one exception, for which we lost track of it.)

The bottom and top surfaces of every beam was polished with a 100 grit size meshed sand paper. This was done to remove the blade marks produced by the band saw. These two surfaces were further smoothed by wiping them with the palm of one hand, such as to melt a thin layer at the surface of the ice, with the aim of removing the bulk of the damage (at the microscopic scale) expected to have occurred during the machining process. This surface preparation (sanding and wiping) was not done for the tests conducted at -0.5C, as these specimens were already so close to melting point that the uppermost surface on all sides had melted after leaving the band saw.

3.3 Test frame

The test frame used for these investigations, shown on the report's front page, was located in CHC's cold room. It comprised two threaded rods joining an upper and a lower assembly. The upper assembly consisted of 1) a load cell, 2) a universal joint and 3) a platen with the two upper application points (with a distance of 101.6 mm between them). The lower assembly consisted of 1) the lower platen with the two load lower application points (with a distance of 304.8 mm between them), and 2) a screw-driven actuator connected onto a gear box, itself activated by an electric motor. The platens were made of aluminum and the load application points were steel cylinders. The ice specimen was located between the lower and the upper platens.

3.4 Temperature

Three *target* test temperatures (what we were aiming for) were selected for these tests: 1) -10^{o}C, 2) -5^{o}C and 3) as close to the melting point as operationally feasible. These temperatures were set using the cold room thermostat, which had a resolution of one degree. The temperature of the air inside the cold room was acquired on an-going basis with a data acquisition system, at a rate of one reading per minute. To ensure that the specimens had equilibrated to the air temperature, the beam preparation procedures described above were done at the target test temperature. In addition, throughout testing, the temperature was also monitored at the center of a 'dummy' ice specimen, with the purpose of obtaining an estimate of what it was *inside* the test specimens (near the centre) during testing. The *effective* test temperatures (those of the ice specimens, as recorded from these probes), were -9.5^{o}C, -5.0^{o}C and -0.5^{o}C.

The refrigeration's defrost cycles caused fluctuations in air temperature up to +/-2^{o}C. Inside the dummy ice specimen, these fluctuations did not exceed +/-0.5^{o}C. So one may assume that temperature fluctuations along the specimens' surface under tensile loading, where failure is expected to have initiated, was between 0.5 and 2^{o}C.

3.5 Ice salinity

Salt content in floating ice covers is known to reduce ice strength, because it tends to be concentrated in brine entrapments, which induce grain size reduction and weaken the material. This is why the strength of sea ice is significantly lower than that of freshwater (lake, river) ice. In order to obtain information on this parameter, several test specimens from different blocks were melted and tested for salinity. All showed values below the salinometer's sensitivity level (0.0 ppt).

3.6 Test procedures

The physical dimensions and the weight of each beam were recorded immediately prior to testing (within a few minutes). The time between specimen preparation and testing did not exceed a few days (and were generally done the same day). In the meantime, they were stored in cooler boxes located inside the cold room. The density of every beam was obtained from the dimensions and weight data. The specimen was then centered onto the lower platen of the test frame, and oriented so that the top of the beam pointed upward. This orientation was to simulate how the ice was loaded in the real case scenario. The motor was then activated, and drove the lower platen up toward the upper assembly, just so as to bring the upper platen to rest onto the specimen. This resulted in a small (about 30 N) pre-load. After final specimen/platens adjustments, motion was resumed at a displacement rate of 0.33 mm/sec (+/- 0.02 mm/sec), until beam failure. This corresponded to a strain rate of about 9.6 x 10^{-4} sec^{-1}. During that time, the load cell output was recorded at a rate of 100 Hz. The peak value was extracted from the load trace (Figure 4). After each test (except in some -10^{o}C tests, where the camera stopped working), photographs were taken of the broken beam. The flexural strength was determined from the peak load and the beam dimensions, using Eq. 1.

4 TEST RESULTS

A total of 56 successful beam tests were done as part of this study. Density and strength information for all tests (white and clear ice) is provided in Table 1, at the three test temperatures, further divided into whether the ice specimens originated from within the skateway or outside of it.

The experimental error for density and strength data, calculated from standard methods, is also included in Table 1 – it is about 11 kg/m^3 for density, and 0.12 MPa for strength. This information provides a means of ‘gauging’ data quality – *i.e.* a relatively large random error indicates that not enough care was taken to reduce uncertainties. For instance, an increase in measurement resolution or a decrease in background noise of the load cell’s output will contribute in decreasing the experimental error. The usefulness of this error is in being able to distinguish between data scatter due to experimental procedures from scatter due to the material’s inherent behaviour. The standard deviation is used in this report to assess overall data scatter.

4.1 Density

Figure 5 shows the difference in average density for all specimens made from clear and white ice, including the standard deviation for each ice type. This information is consistent with a higher amount of air entrapment expected in the white ice. The plot also includes the density of pure ice (zero air content), for the purpose of comparison. Note that the white ice density is below the 880 kg/m^3 threshold above which all ice is considered ‘full strength’ ice (see discussion in Masterson, 2009, p. 104).

4.2 Flexural strength of white and clear ice

Figure 6 illustrates the ice strength for both the white and the clear ice, at the three different test temperatures. White ice was weaker than clear ice by 36%, 21% and 51% at test temperatures of -9.5^{o}C, -5.0^{o}C and -0.5^{o}C, respectively. Clear ice was strongest at -9.5 ^{o}C and weakest at -0.5^{o}C. Interestingly, the strength of the white ice at -9.5^{o}C was not significantly different from that at -5.0^{o}C. The standard deviation, obtained from the pooled values for each ice type, is shown in that figure.

4.3 Flexural strength vs density

Figure 7 illustrates the relationship between ice strength and ice density at each of the three test temperatures. These plots display a positive correlation between these two parameters.

4.4 Flexural strength vs location

Figure 8 illustrates the difference in flexural strength between ice taken from inside the skating zone and outside of it. This plot incorporates the combined average strength of both clear and white ice. At each of the three experimental temperatures, the ice inside the skating zone was weaker than that outside of it by 27%, 23% and 37% at test temperatures of -9.5^{o}C, -5.0^{o}C and -0.5^{o}C, respectively. The standard deviation, obtained from the pooled values at each of the two locations, is shown in that figure.

4.5 Flexural strength vs temperature

The foregoing already showed that the flexural strength generally decreases with increasing temperature. In Figure 9, the average strength for white and clear ice at the three test temperatures are incorporated into a data compilation by Timco and O'Brien (1993, Fig. 1). It indicates a progressive reduction in strength toward the melting point for both ice types. For the white ice, most of the strength reduction took place between -5 and -0.5^{o}C. This figure shows a general agreement between the data produced during this study and those reported elsewhere.

A linear regression in Figure 9 through both ice types – when strength values for clear and white ice are averaged at each of the three test temperatures – has a slope of -0.1 MPa/^{o}C. Considering that the uncertainty in specimen surface temperature varies between 0.5^{o}C and 2^{o}C, as discussed earlier (section 3.4), the maximum experimental error is 0.2 MPa. This error, combined with that shown in Table 1 for strength, are substantially lower than the standard deviation, implying that data scatter mostly reflects material variability.

5 CONCLUSION

The beams made from white ice were consistently weaker than those made from clear ice. This strength reduction was 36%, 21% and 51% at test temperatures of -9.5^{o}C, -5.0^{o}C and -0.5^{o}C, respectively. Moreover, the ice inside the skating zone was weaker than that outside of it by 27%, 23% and 37% at each of these three temperatures, respectively. In all cases, however, the average values of the data sets were within one standard deviation of each other, suggesting considerable variability in material response.

6 ACKNOWLEDGEMENTS

Garry Timco initiated the work agreement between CHC-NRC and BMT Fleet Technology Ltd. Razek Abdelnour visited the test facility and provided useful feedback. He is also thanked for arranging logistical support on the ice. John Marquardt looked after ice harvesting and helped out with the experimental set-up. Bob Frederking shared his views on testing procedures and made helpful comments on an early draft of this report.

7 REFERENCES

Frederking, R.M.W. and Svec, O.J. (1985) Stress-relieving techniques for cantilever beam tests in an ice cover. Cold Regions Science and Technology, Vol. 11, pp. 247-253.

Masterson, D.M. (2009) State of the art of ice bearing capacity and ice construction. Cold Regions Science and Technology, Vol. 58, pp. 99-112.

Svec, O.J., Thompson, J.C. and Frederking, R.M.W. (1985) Stress concentrations in the root of an ice cover cantilever: Model tests and theory. Cold Regions Science and Technology, Vol. 11, pp. 63-73.

Timco, G.W. and O'Brien, S. (1994) Flexural strength equation for sea ice. Cold Regions Science and Technology, Vol. 22, pp. 285-298.

TABLES

Table 1: Test grid and data summary.

Temperature: -0.5 +/- 0.5C									
White ice	Density kg/m 3	Error kg/m 3	Strength MPa	Error MPa	Clear ice	Density kg/m 3	Error kg/m 3	Strength MPa	Error MPa
INSIDE skating zone					INSIDE skating zone				
E1a	885	11	0.15	0.12	E2a	959	12	0.62	0.12
E1b	884	11	0.48	0.13	E2b	903	12	0.88	0.13
E1c	894	11	0.46	0.12	E2c	899	12	0.90	0.13
E1d	856	11	0.45	0.13	E2d	905	12	0.61	0.13
E1e	859	11	0.38	0.14	E3d	903	11	1.25	0.12
E1f	865	12	0.37	0.14					
OUTSIDE skating zone					OUTSIDE skating zone				
F1a	844	11	0.67	0.14	F2a	914	12	1.37	0.13
F1b	862	11	0.67	0.12	F2b	886	11	1.39	0.12
F1c	866	11	0.76	0.12	F2c	903	12	0.88	0.13
F1d	851	11	0.53	0.12	F2d	898	11	1.39	0.12
					F2e	899	12	0.83	0.12
Temperature: -5.0C +/- 0.5C									
White ice	Density kg/m 3	Error kg/m 3	Strength MPa	Error MPa	Clear ice	Density kg/m 3	Error kg/m 3	Strength MPa	Error MPa
INSIDE skating zone					INSIDE skating zone				
G1a	873	11	1.19	0.13	E2e	885	11	1.41	0.13
G1b	877	11	0.83	0.12	E2f	900	12	1.42	0.14
G1c	866	11	1.41	0.13	E3e	873	11	1.64	0.13
G1d	846	11	0.77	0.12	E3f	882	11	1.49	0.13
OUTSIDE skating zone					OUTSIDE skating zone				
F1e	857	11	1.34	0.13	F2f	876	11	1.62	0.13
F1f	861	11	1.64	0.13	F2g	894	11	1.52	0.12
F1h	853	11	1.53	0.14	F2h	882	11	1.63	0.13
F1i	851	11	1.57	0.13	F2i	907	12	2.34	0.15
Temperature: -9.5C +/- 0.5C									
White ice	Density kg/m 3	Error kg/m 3	Strength MPa	Error MPa	Clear ice	Density kg/m 3	Error kg/m 3	Strength MPa	Error MPa
INSIDE skating zone					INSIDE skating zone				
G1e	870	11	1.49	0.13	E2g	882	11	1.78	0.13
G1f	864	11	1.34	0.13	G2a	903	12	1.67	0.13
G1g	864	11	1.39	0.13	G2b	898	12	1.53	0.13
G1h	836	11	1.07	0.12	G2c	899	12	1.37	0.13
G1i	857	11	0.97	0.13					
G1j	882	11	1.28	0.13					
G1k	863	11	1.51	0.13					
G1l	851	11	1.23	0.12					
OUTSIDE skating zone					OUTSIDE skating zone				
F1j	871	11	1.52	0.13	F2j	896	12	2.67	0.15
F1k	855	11	1.06	0.13	F2k	886	11	2.73	0.14
H1a	879	11	1.44	0.14	F2l	910	12	2.83	0.16
H1b	863	11	1.48	0.14					
H1c	854	11	1.42	0.14					

FIGURES

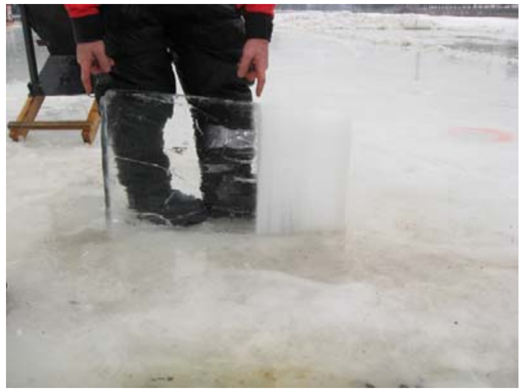

Figure 1: Left) Extracting the ice with a chain saw. Right) 'Clear' zone and 'white' zone inside one block (the finger points at the boundary between the two zones).

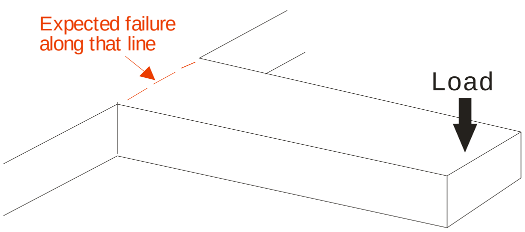

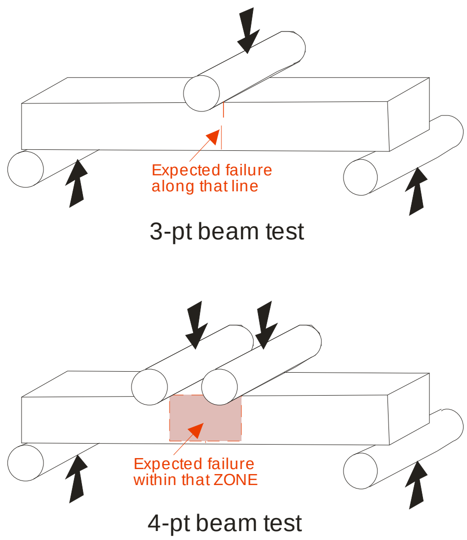

Figure 2: Left) Cantilever beam test. Right) '3-pt' versus '4-pt' beam tests. See text for discussion.

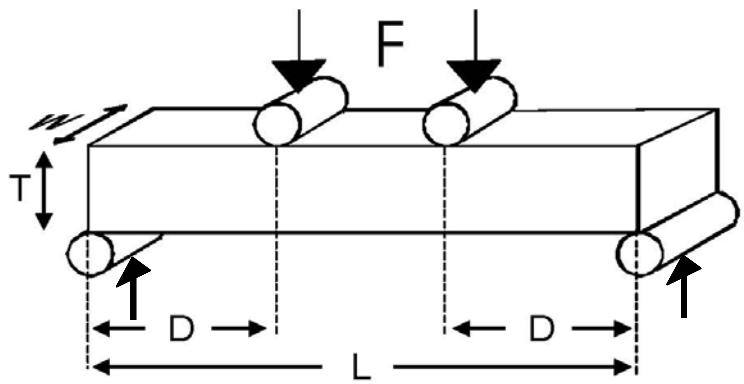

Figure 3: Parameters used for flexural strength determination.

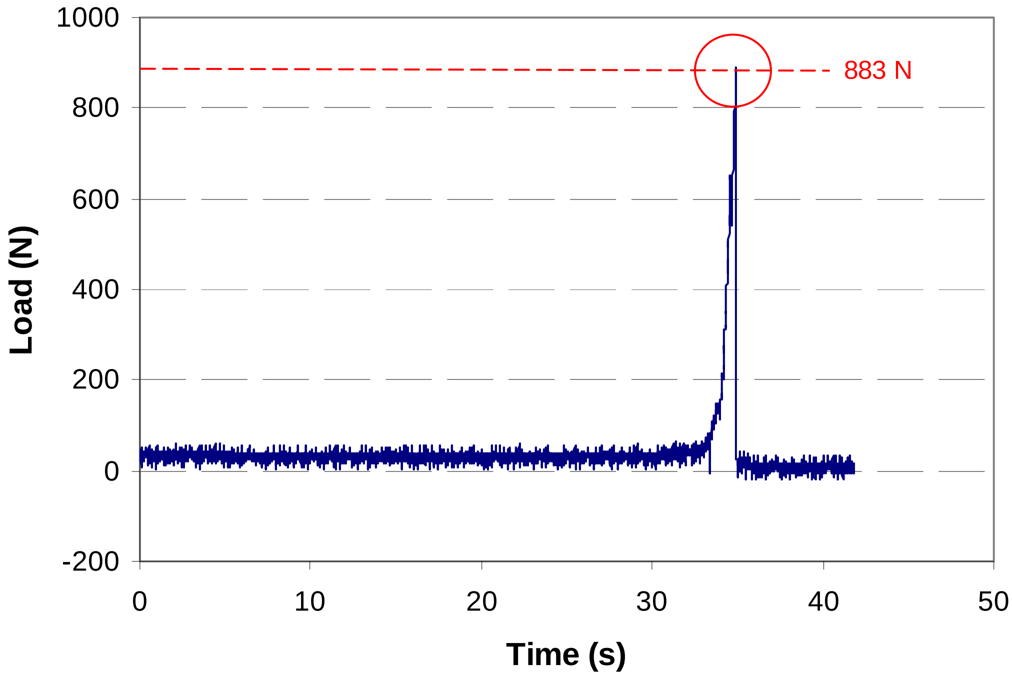

Figure 4: Example of a peak load (from test E2g). The peak load for this test, required for beam failure, was 883 N. The small pre-loading event described in the test procedures is shown prior to that event. The electrical noise (+/- 50 N) was taken into account to derive the experimental error.

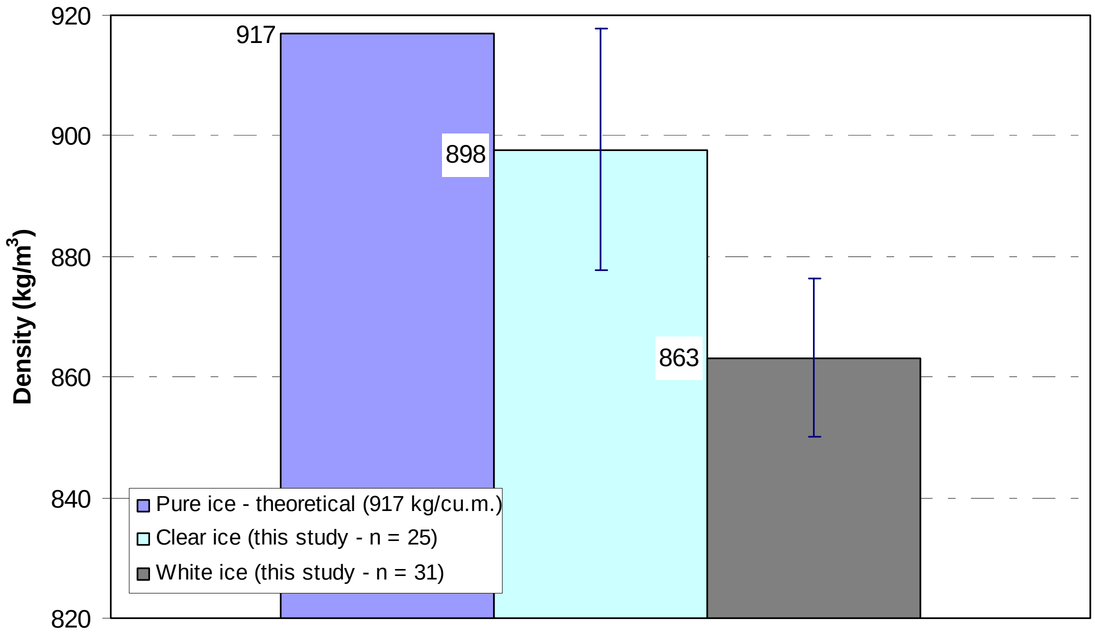

Figure 5 : A comparison between density of pure ice with that of the 'clear' and the 'white' ice investigated in this study. The standard deviation is indicated for the two latter.

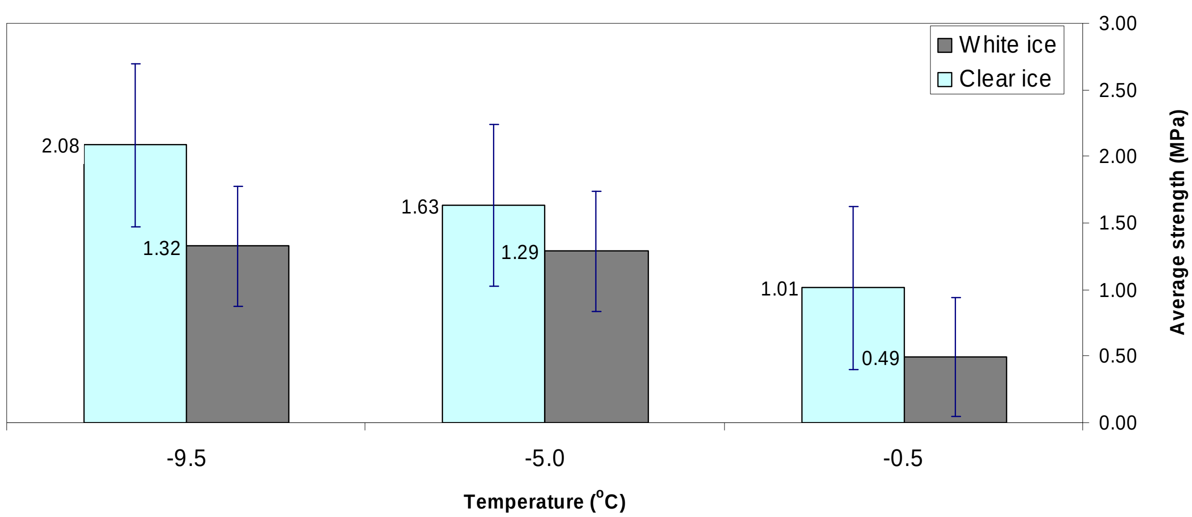

Figure 6: Average strength, at each of the three test temperatures, for the white and the clear ice. The standard deviation for each of the two data sets is indicated (0.45 and 0.60 MPa for white and clear ice, respectively).

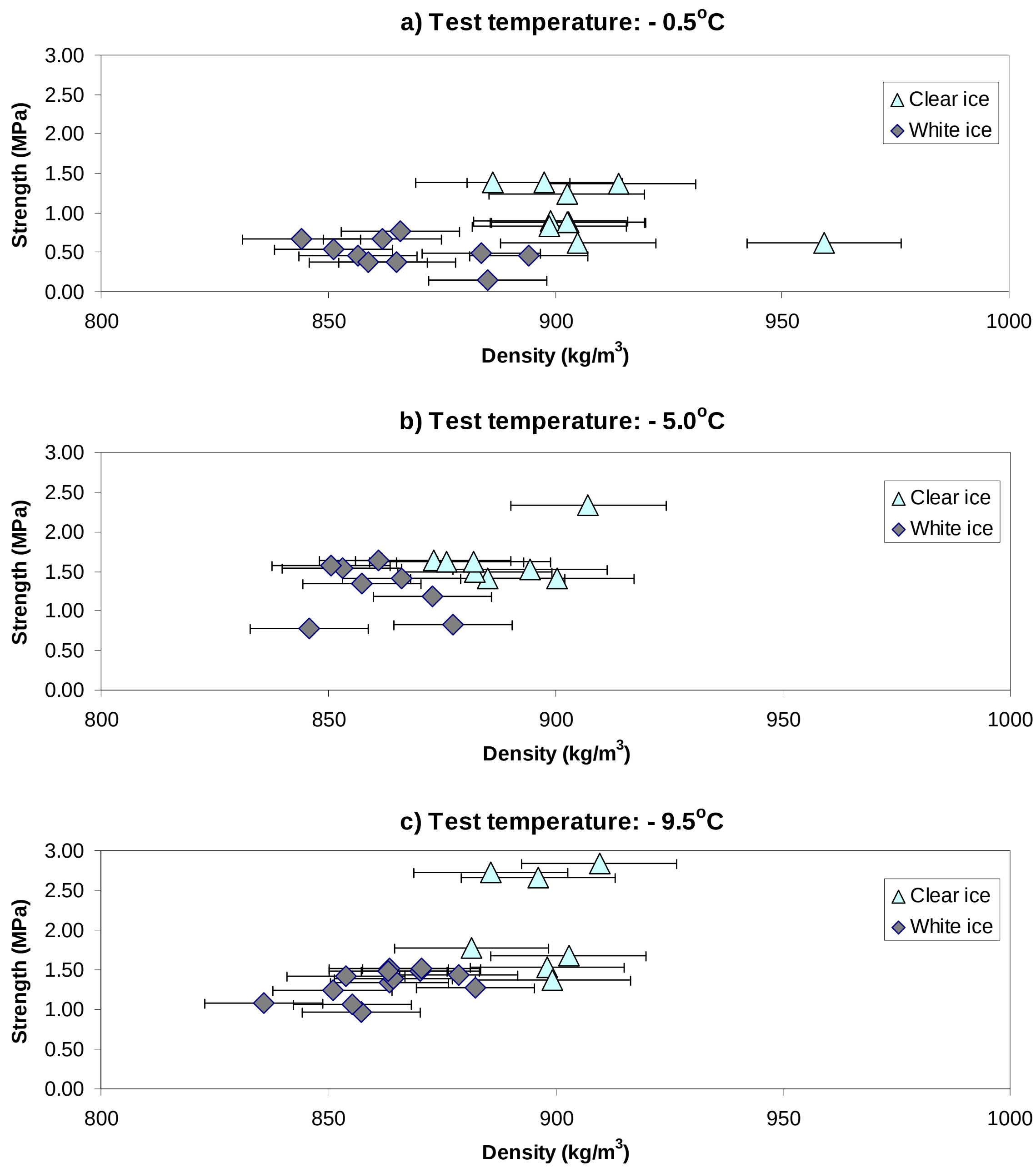

Figure 7: Strength variation as a function of density: a) -0.5°C, b) -5.0°C, c) -9.5°C. The experimental error for the density is indicated (the error for the strength does not exceed the size of the symbols).

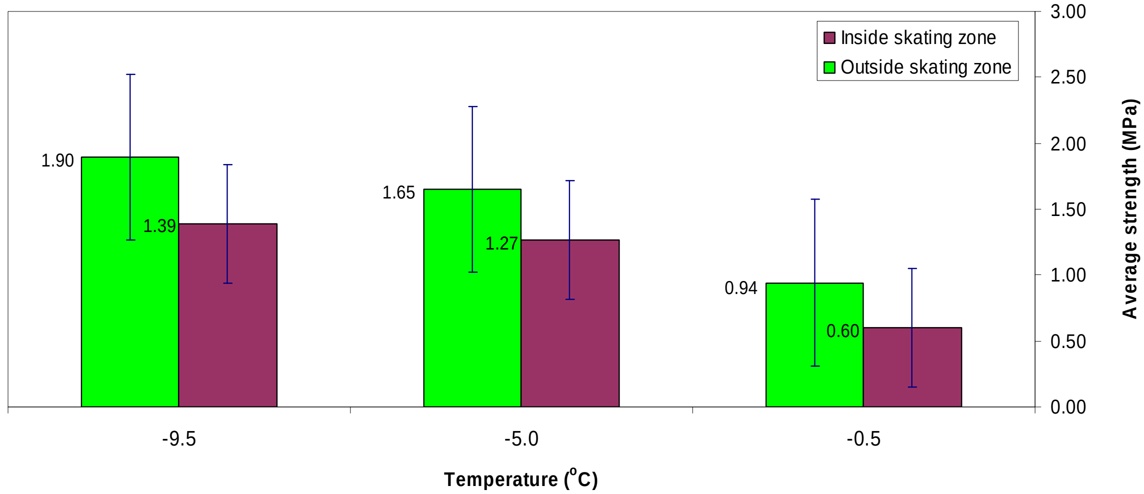

Figure 8: Average strength, at each of the three test temperatures, for the ice from within the skating zone and outside of it. The standard deviation for each of the two data sets (0.45 and 0.63 MPa for inside and outside, respectively) is indicated.

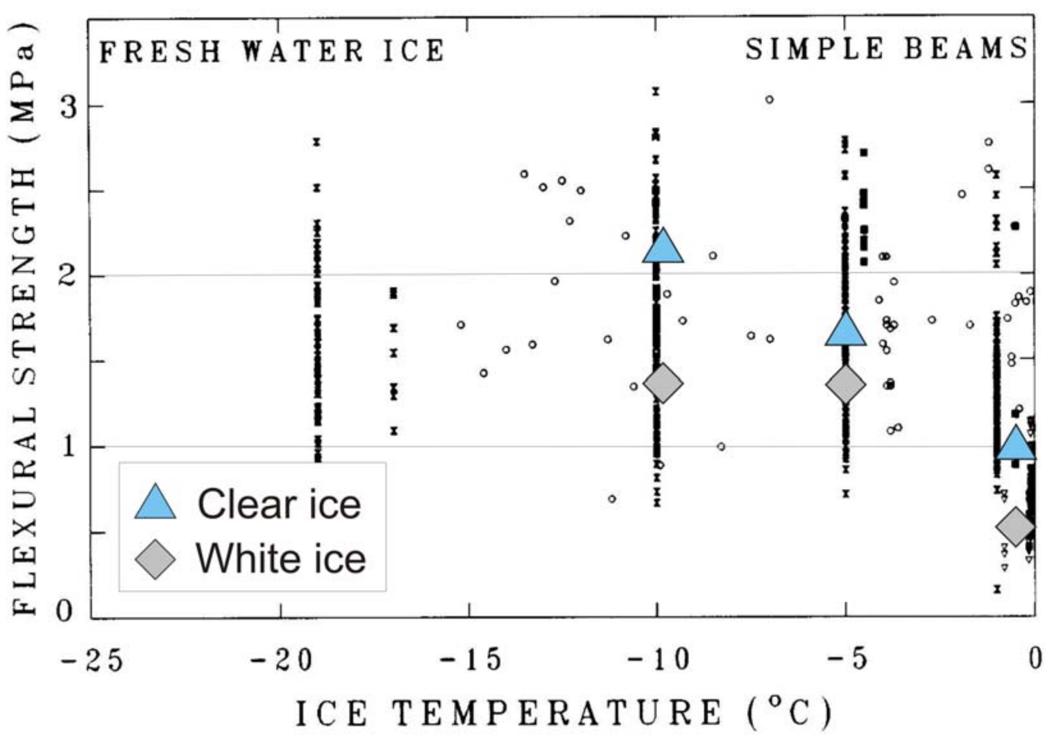

Figure 9: The average strength at each of the test temperature is plotted on a compilation by Timco and O'Brien (1994, Fig. 1).